Circular RNAs exhibit limited evidence for translation, or translation regulation of the mRNA counterpart in terminal hematopoiesis

BENOIT P. NICOLET,[1,2] SJOERT B.G. JANSEN,[3] ESTHER HEIDEVELD,[1] WILLEM H. OUWEHAND,[3] EMILE VAN DEN AKKER,[1] MARIEKE VON LINDERN,[1] and MONIKA C. WOLKERS[1,2]

[1]Department of Hematopoiesis, Sanquin Research and Landsteiner Laboratory, Amsterdam UMC, University of Amsterdam, 1066CX Amsterdam, The Netherlands

[2]Oncode Institute, Utrecht, The Netherlands

[3]Department of Haematology, University of Cambridge and NHS Blood and Transplant, Cambridge CB2 0AW, United Kingdom

ABSTRACT

Each day, about 10^{12} erythrocytes and platelets are released into the bloodstream. This substantial output from hematopoietic stem cells is tightly regulated by transcriptional and epigenetic factors. Whether and how circular RNAs (circRNAs) contribute to the differentiation and/or identity of hematopoietic cells is to date not known. We recently reported that erythrocytes and platelets contain the highest levels and numbers of circRNAs among hematopoietic cells. Here, we provide the first detailed analysis of circRNA expression during erythroid and megakaryoid differentiation. CircRNA expression not only significantly increased upon enucleation, but also had limited overlap between progenitor cells and mature cells, suggesting that circRNA expression stems from regulated processes rather than resulting from mere accumulation. To study circRNA function in hematopoiesis, we first compared the expression levels of circRNAs with the translation efficiency of their mRNA counterpart. We found that only one out of 2531 (0.04%) circRNAs associated with mRNA-translation regulation. Furthermore, irrespective of thousands of identified putative open reading frames, deep ribosome-footprinting sequencing, and mass spectrometry analysis provided little evidence for translation of endogenously expressed circRNAs. In conclusion, circRNAs alter their expression profile during terminal hematopoietic differentiation, yet their contribution to regulate cellular processes remains enigmatic.

Keywords: circRNA; translation; translation regulation; red blood cells; platelets; megakaryocytes

INTRODUCTION

Each hour, millions of red blood cells (RBC) and platelets are produced in the bone marrow and released into the bloodstream. Their production is mediated from erythroid and megakaryoid progenitors. The generation of these progenitors from hematopoietic stem cells is a highly orchestrated process. Tight regulation is obtained by the coordinated expression of transcription factors, long noncoding RNAs, and micro-RNAs (Petriv et al. 2010; Luo et al. 2015; Goode et al. 2016). Recently, we showed that also circular RNAs (circRNAs) are abundantly expressed in hematopoietic cells, and that their expression alters during differentiation (Nicolet et al. 2018).

CircRNAs are single stranded, circular RNA molecules that are generated from pre-mRNA transcripts through back-splicing (Hansen et al. 2013; Memczak et al. 2013; Chen 2016). Back-splicing is driven by the classical spliceosome machinery at canonical splice sites (Ashwal-Fluss et al. 2014), and circularization is mediated by pairing of complementary sequences, typically Alu elements, which are found in flanking introns. The pairing of Alu elements is regulated by RNA-binding proteins such as ADAR, DHX9, and NF90 (Rybak-Wolf et al. 2015; Aktaş et al. 2017; Li et al. 2017). CircRNA can contain both intron and exon segments. While intronic circRNA are mostly retained in the nucleus (Li et al. 2015), exonic circRNA undergo nuclear translocation in a size-dependent manner (Jeck et al. 2013; Huang et al. 2018). In the cytoplasm, circRNAs are found to be exonuclease-resistant (Suzuki et al. 2006). In addition, circRNA

Corresponding authors: m.wolkers@sanquin.nl, b.nicolet@sanquin.nl

Article is online at http://www.rnajournal.org/cgi/doi/10.1261/rna.078754.121. Freely available online through the *RNA* Open Access option.

lack the 3′ polyadenylation tail, which renders them more stable than linear RNA (Enuka et al. 2016).

Many functions have been attributed to circRNAs. CircRNAs were suggested to act as transcriptional activators (Li et al. 2015; Zhang et al. 2016), or to serve as RNA-binding protein cargo (Hentze and Preiss 2013). CircRNAs can also act as an miRNA "sponge," a feature that is to date limited to about 10 circRNAs genome-wide in humans (Guo et al. 2014; Piwecka et al. 2017; Stagsted et al. 2019). In addition, circRNA-mediated regulation of mRNA translation has been proposed in cell lines (Sun et al. 2019; Wu et al. 2019; Li et al. 2020). Lastly, it was shown with over-expression constructs in cell lines (Legnini et al. 2017; Yang et al. 2017), and from exemplary circRNAs in Drosophila and human cell lines that circRNA can be translated into protein (Pamudurti et al. 2017; Liang et al. 2019). How these findings translate to endogenous circRNA expression during human hematopoietic differentiation is not known.

We and others have observed that RBCs and platelets had the highest numbers and highest circRNA content of all analyzed mature cell types in humans (Alhasan et al. 2016; Maass et al. 2017; Nicolet et al. 2018). However, the origin of these high circRNA levels is not known and has thus far been attributed to transcriptome degradation (Alhasan et al. 2016). In addition, the function of these circRNA in blood cell development remains unknown.

In the study presented here, we provide a detailed and comprehensive analysis of circRNA expression in erythroid and megakaryoid development. We identified >20,000 circRNAs in erythroid differentiation and >12,000 in megakaryoid differentiation. The expression of circRNAs alters dramatically upon enucleation and platelet formation, and only partially (~40%) follows mRNA expression in differentiating blood cells. Integration of RNA-seq and Ribo-seq data revealed that circRNA-mediated regulation of mRNA translation is not the main mode of action during megakaryocytic maturation. Furthermore, ribosome-footprinting analysis and mass spectrometry analysis demonstrated that translation of endogenous circRNAs may occur in reticulocytes, megakaryocytes, and/or platelets; however, this is not a frequent event. In conclusion, even though circRNAs are highly prevalent in erythroid and megakaryoid development, their mode of action and activity in hematopoietic cells does not follow the proposed models and thus remains to be defined.

RESULTS

CircRNA are abundant during erythropoiesis

We first investigated if and how circRNA expression alters during terminal erythropoiesis. To this end, we examined paired-end RNA sequencing data of erythroblasts isolated from four donors that were cultured for 12 d under differentiating conditions, and that were harvested on each day between days 0 and 7, in addition to days 9 and 12 (Fig. 1A; Heshusius et al. 2019). This in vitro differentiation model resulted in overall gene expression patterns that closely resembled that of ex vivo isolated cells (Supplemental Fig. S1A; Supplemental Table S1; Heshusius et al. 2019). Also, physical properties such as hemoglobin content, oxygen association, and dissociation capacity and deformability matched those of ex vivo red blood cells (Heshusius et al. 2019).

The average sequencing depth of 30 million reads identified on average 27.3 million mapped reads. To detect, quantify, and annotate circRNAs from chimeric reads, we used our established pipeline (Nicolet et al. 2018) that is based on the two algorithms DCC (Cheng et al. 2015) and CircExplorer2 CE2 (Zhang et al. 2014; see Materials and Methods section). With a "low-confidence" cutoff of at least two reads in at least one sample at any time of harvest, 20,931 circRNAs were co-detected by DCC and CE2 (Fig. 1B; Supplemental Table S2). Based on mRNA splicing annotations and circRNA junction reads, the estimated number of exons/circRNA was 5.58 in differentiating erythroblasts (median = 4 exons/circRNA; Fig. 1C). The putative length of circRNAs was 846.14 nt (median = 619 nt; Fig.

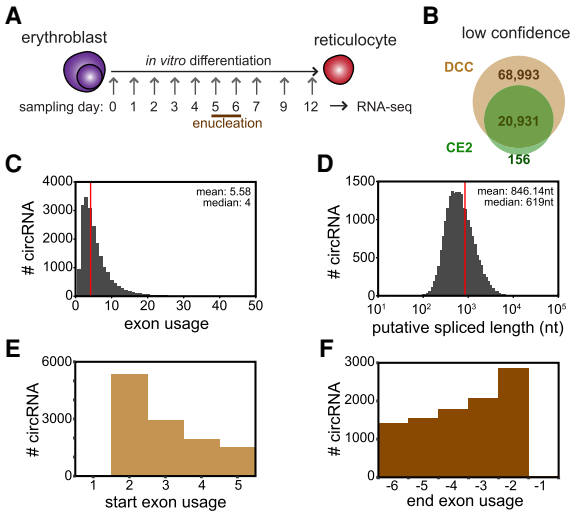

FIGURE 1. CircRNAs are abundant during in vitro erythroid differentiation. (*A*) Erythroblast progenitors were cultured for 12 d under differentiation conditions, as in Heshusius et al. (2019). Samples were taken at indicated days of differentiation, and RNA-seq was performed ($n = 4$ donors). (*B*) CircRNA detection using DCC and CircExplorer2 (see Materials and Methods) to identify "low-confidence" (circRNA with at least two reads in at least one sample) in all compiled samples from *A*. The intersection of the circles represents the co-detected circRNAs with both tools. (*C*,*D*) Characterization of low-confidence circRNA. (*C*) Putative exon usage and (*D*) putative spliced length, using splicing annotations from linear isoforms. (*E*,*F*) Characterization of (*E*) start and (*F*) end exon usage by "low-confidence" circRNAs, based on the circRNA junction positions and canonical mRNA splicing annotation.

1D). In line with our previous work (Nicolet et al. 2018), circRNAs preferentially use the second exon of a linear transcript as the first circular exon (Fig. 1E), a bias that is not as pronounced for the last circularized exon (Fig. 1F). Thus, circRNAs are abundantly expressed during erythropoiesis.

CircRNA levels increase at enucleation

To define how circRNA expression related to the expression of other transcripts during erythroid differentiation, we quantified the overall expression of protein-coding transcripts (mRNA; transcripts per kilobase per million [TPM] > 0.1), noncoding transcripts (ncRNA; TPM > 0.1), and circRNA transcripts (low-confidence circRNA; RPM). We detected 19,449 mRNA-, 10,753 ncRNA-, and 4526 circRNA-producing genes (Fig. 2A). We also quantified the diversity of transcripts expressed during erythrocyte differentiation. At the early time points (i.e., up to day 5), erythroblasts mainly expressed mRNA and ncRNA transcripts (Fig. 2B). These numbers steadily decreased over time and were reduced by 82.96% and 76.45%, respectively, at day 12 compared to day 0 (Fig. 2B). In contrast, the number of circRNA transcripts substantially increased by a ~3.8-fold from day 6 onward compared to day 0, and circRNA transcripts even surpassed the number of ncRNA transcripts at day 8 (Fig. 2B). This steep increase of circRNAs coincided with the enucleation rate (Fig. 2C).

To measure the differential expression of circRNAs during erythropoiesis, we focused on "high-confidence" circRNAs, that is, a given circRNA is detected at least twice in all four donors at an individual time-point. This filter identified 950 circRNAs that were co-detected by DCC ($n = 1163$) and CE2 ($n = 958$; Fig. 2D; Supplemental Table S2). Pearson's correlation coefficient of all measured time points during erythropoiesis revealed two main clusters of circRNAs that were primarily expressed early (day 0–5), or late during differentiation (day 6–12; Fig. 2E). In fact, a heatmap representation of high-confidence circRNA expression showed a massive increase in circRNA expression from day 6 onward (Supplemental Fig. S1B). When we compared all days to day 0 (Fig. 2F), 708 circRNAs (74.5%) were differentially expressed (*P*-adjusted <0.05; Supplemental Table S2). Of these, all but one circRNA, *circ-FIRRE* (Supplemental Fig. S1C), significantly increased their expression levels from day 6 onward (Fig. 2F; Supplemental Table S2). Of note, the expression of the proliferation marker MKI67 (KI-67) in nucleated blood cells did not correlate with the circRNA expression ($R^2 = 0.134$; $P = 0.113$; Supplemental Fig. S1D).

We next investigated how circRNA expression related to the expression of their mRNA counterparts in erythroid differentiation. To this end, we used the build-in linear detection of DCC, as described previously (Nicolet et al. 2018). Briefly, as a circRNA can only be detected and quantified by their junction read, linear detection was performed at the same positions (start and end position of circRNA). The circular-over-linear expression ratio (CLR) was calculated for each "high-confidence" circRNA, averaged across the four biological replicates for each time-point (Supplemental Fig. S1E; Supplemental Table S2). Of note, as circRNA expression varies per culture day, we only consider the CLR of circRNA that are expressed at a given time point (CLR > 0). This filtering step may thus introduce a slight inflation of the average CLR at early time points (i.e., day 0–5). Between day 0

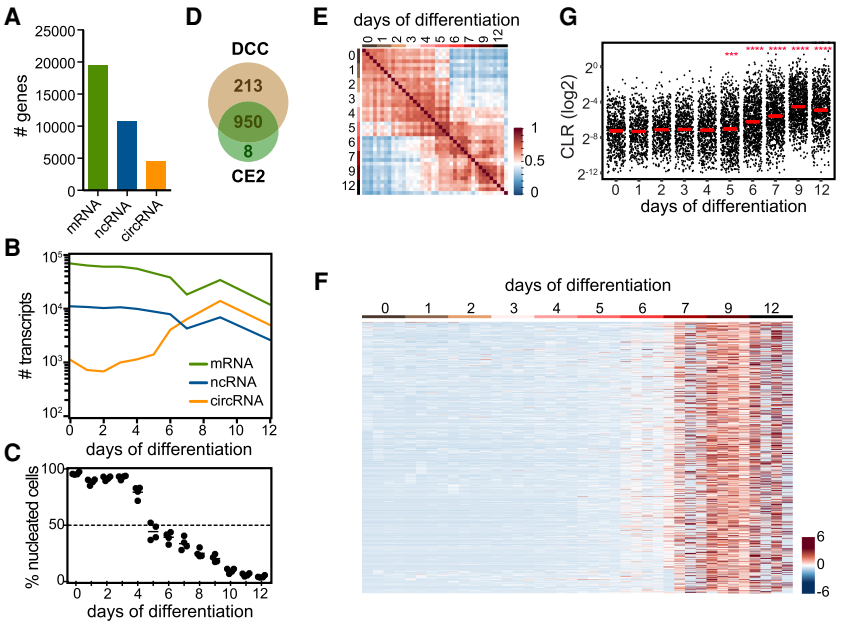

FIGURE 2. CircRNA expression increases at enucleation of erythroid cells. (*A*) Number of genes encoding mRNA, noncoding RNA (ncRNA), and circRNA, and (*B*) the number of transcripts detected during erythroid differentiation (cutoff: >0.1 TPM for mRNA and ncRNA; low-confidence circRNA). (*C*) Percentage of enucleated cells at indicated time point ($n = 4$ donors; data from Heshusius et al. 2019). (*D*) CircRNA detection using DCC and CircExplorer2 (see Materials and Methods) from RNA-seq data generated from Figure 1. The intersection of the circle represents the co-detected circRNA referred to as "high confidence" (circRNA with at least two reads in all four biological replicates of one time-point). (*E*) Pearson's sample-correlation coefficient map of "high-confidence" circRNA expression. (*F*) Heatmap of the differentially expressed "high-confidence" circRNA ($n = 708$; *P*-adjusted <0.05) corrected for sequencing depth (RPM). (RPM) Reads per million mapped (linear) reads. (*G*) Circular-over-linear ratio (CLR) was calculated for "high-confidence" circRNAs during erythropoiesis, median is indicated in red. Differences were assessed by two-sided *t*-test with Benjamini–Hochberg *P*-value adjustment, all compared to day 0. (***) Padj < 0.001, (****) Padj < 0.0001.

and day 5 of erythropoiesis, the mRNA expression was higher compared to circRNA, as no circRNAs showed a CLR above one. Only from day 6 onward, 25 circRNAs showed a CLR > 1, that is, circRNA expression is higher than that of their linear counterpart. Also, the overall CLR increased from day 6 onward and peaked at day 9 with a 7.3-fold increase compared to day 0 (Fig. 2G). In conclusion, circRNA expression substantially alters at enucleation and can reach levels that are higher than those of their mRNA counterpart.

CircRNA expression alters from megakaryocytes to platelets

We next investigated how circRNAs are expressed during megakaryopoiesis and in platelets, which are formed and released into the bloodstream by mature megakaryocytes. We performed RNA-seq analysis of three donors on purified immature CD41a$^+$ CD42b$^-$ (CD42–) and mature CD41a$^+$ CD42b$^+$ (CD42+) megakaryocytes that were cultured from cord blood CD34$^+$ progenitors (see Materials and Methods; Fig. 3A). Again, also the gene expression of cultured MKs closely resembled that of previous studies (Supplemental Fig. S1A; Supplemental Table S1). The average sequencing depth of 84.4 million reads per sample resulted in on average 74.6 million mapped reads to the genome. CircRNA detection with DCC and CE2 co-detected 12,809 circRNAs with low-confidence filtering (Fig. 3B; Supplemental Table S3). To define the relation of mRNA, ncRNA, and circRNA expression during MK differentiation, we quantified the number of genes expressing these transcripts. We also included our previous analysis of circRNA expression in platelets to this analysis pipeline (Nicolet et al. 2018). Similar to erythropoiesis, the number of expressed mRNA and ncRNA genes decreased in particular in anucleate platelets, where the number of circRNA expressing genes increased by a 2.1-fold compared to MKs (Supplemental Fig. S2A). Furthermore, with 47,654 low-confidence circRNAs detected, platelets had the highest diversity of circRNA transcripts (average sequencing depth in million mapped reads: platelet = 40.6; MK = 74.6; Fig. 3C). In megakaryocytes, the estimated exon usage with a mean of 4.57 exon/circRNA (median = 4) and the putative spliced length with a mean of 663.9 nt/circRNA (median thinsp;= 483 nt), was slightly lower than that of circRNAs in erythropoiesis (Fig. 1C,D; Supplemental Fig. S2B,C). Yet, a preference for the second exon usage for circularization was apparent (29.2% of circRNA), with no overt preference of the last exon (14.2% of circRNA; Supplemental Fig. S2D,E).

To determine the differential circRNA expression in MKs, we focused on the 2531 high-confidence circRNAs (Supplemental Fig. S2F). Pearson's sample-correlation coefficient revealed a strong kinship between CD42– and CD42+ MK (Fig. 3D). Yet, differential expression analysis of circRNA, identified 287 out of 2531 (11.34%) circRNAs, including the key transcription factor for MK differentiation FLI1 (*P*-adjusted <0.05 and $\log_2$ fold change >0.5; Fig. 3E; Supplemental Table S3). All differentially expressed circRNA were found in CD42+ MK. Platelets, however, showed an overall distinct expression pattern of

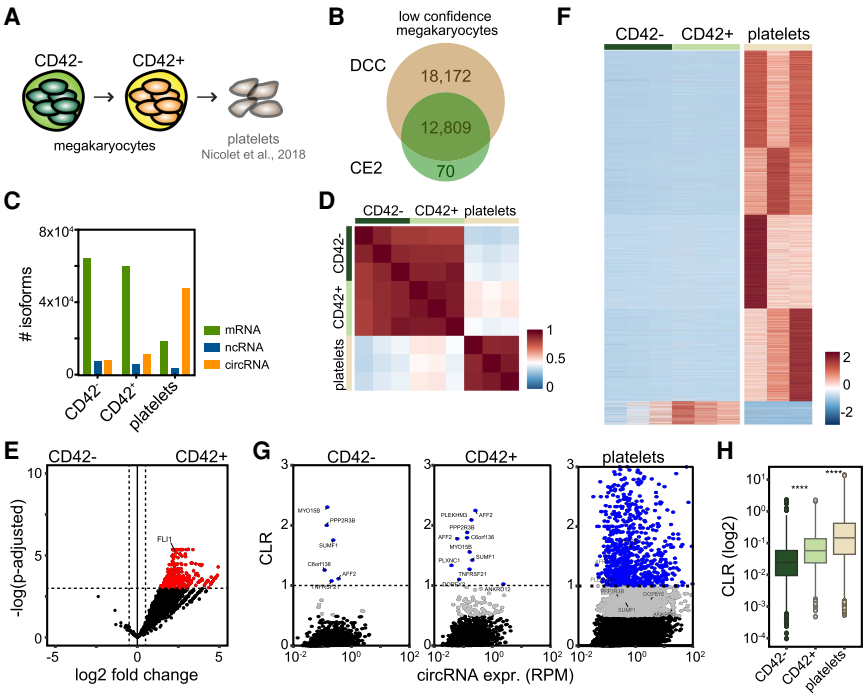

FIGURE 3. CircRNA expression during megakaryocyte differentiation. (*A*) Diagram representing in vitro differentiation from CD42– and CD42+ megakaryocytes ($n = 3$ per population) to platelets (Nicolet et al. 2018). (*B*) CircRNA detection in CD42– and CD42+ megakaryocytes from RNA-seq data, using DCC and CircExplorer2. The intersection of the circle represents the co-detected "low-confidence" circRNAs. Of note, platelet data were not included for circRNA detection in megakaryocytes. (*C*) Number of mRNA, noncoding RNA (ncRNA), and circRNA transcripts detected during megakaryoid differentiation (>0.1 TPM for mRNA and ncRNA; low-confidence circRNA). (*D*) Pearson's sample-correlation coefficient map between CD42– and CD42+ megakaryocytes, and platelets (high-confidence circRNA expression). (*E*) Volcano plot showing the differential expression of high-confidence circRNA between CD42– (*left*) and CD42+ megakaryocytes (*right*; $n = 287$; *P*-adjusted <0.05 and LFC > 0.5, *Z*-score of reads per million mapped reads). (*F*) Heatmap of high-confidence circRNAs detected in megakaryocytes and platelets. (*G*,*H*) Circular-over-linear ratio (CLR) was calculated for CD42– and CD42+ megakaryocytes and plotted against circRNA expression (*G*) or (*H*) compared between populations. Differences were assessed in *H* by two-sided *t*-test *P*-value adjustment using the Benjamini–Hochberg procedure; (****) *P*adj < 0.0001.

circRNAs compared to the two megakaryocytic populations (Fig. 3D,F; Supplemental Table S3). Interestingly, not only the overall expression of circRNAs increased as CD42− MK matured toward platelets, but the overall CLR increased by ~2.1-fold during MK differentiation and by 3.11 between CD42+ MK and platelets (Fig. 3G,H; Supplemental Table S3; Nicolet et al. 2018). Thus, circRNA are expressed and increase as megakaryocytes mature, yet substantially differ from circRNA expression in platelets.

CircRNA expression can be independent of mRNA expression

We next studied how changes in circRNA expression related to changes in expression of the linear mRNA counterpart. To this end, we calculated the $\log_2$ fold change (LFC) in circRNA and mRNA expression in erythroid cells. We isolated five groups based on circRNA and mRNA expression changes (LFC > 0.5): *group 1*: decreased in circRNA levels and decreased in mRNA levels; *group 2*: increased circRNA levels and decreased mRNA levels; *group 3*: increased circRNA levels and unchanged mRNA levels; *group 4*: increased circRNA levels and increased mRNA levels; *group 5*: unchanged circRNA levels; *group 6*: decreased circRNA and increased mRNA levels. When we compared the circRNA expression with the mRNA expression before enucleation, that is, day 0 with day 5, we found that of 37.6% circRNAs, the changes (up or down) coincided with that of the mRNA counterpart (Fig. 4A; group 1 [down] and 4 [up]). Of the 35.4% circRNAs that increased their expression (groups 2 and 3), 18.3% of the mRNA counterpart decreased its expression (Fig. 4A; group 2), and 17.1% remained unchanged (group 3). We also detected circRNAs whose expression levels remained unchanged throughout the first 5 d of differentiation (group 5; 24.6%).

We then asked how the circRNA and mRNA expression relates upon enucleation. We compared the LFC of circRNA and mRNA expression of day 0 with that of day 9 of erythrocyte differentiation (Fig. 4B). The overall high-confidence circRNA expression increased at day 9 compared to day 0 by ~20 times from 32 to 651 identified circRNAs (Fig. 4B). Owing to this increase, only 1.3% of circRNA did not alter, and 1.6% decreased their expression levels (Fig. 4B; groups 5 and 1, respectively). 48.6% of circRNAs showed an increase or decrease of expression in line with their mRNA counterpart (Fig. 4B; groups 1 and 4). Close to half (50.1%) of the circRNAs increased their expression levels, whereas the mRNA expression of the linear counterpart decreased or remained unchanged (Fig. 4B; group 2; 31.5%, and group 3; 18.5%, respectively). When comparing day 5 or day 9 to day 0 of differentiation, we detected only 13 and 0 circRNAs, respectively, with decreased circRNA expression levels for which the mRNA levels increased (Fig. 4A,B; group 6). We next questioned how the changes in circRNA expression related to mRNA changes measured at the circRNA positions throughout the entire erythroid differentiation process. We used the mRNA expression to define clusters and matched these to the circRNA expression (Fig. 4C). Whereas mRNA expression is more heterogeneously expressed, circRNA expression primarily increased around enucleation around day 6 (Fig. 4C). Thus, the majority of circRNA do not follow the expression pattern of their linear counterpart in differentiating RBCs prior and after enucleation, indicating that circRNA expression in differentiating erythroid cells can be independent of mRNA expression.

We also compared the changes in circRNA and mRNA expression between CD42− and CD42+ megakaryocytes. The magnitude of the overall expression changes in MK was lower compared to erythroblasts (~7.6 LFC mRNA and ~7.7 LFC circRNA in MK, compared to ~16.7 LFC mRNA and ~13.9 LFC circRNA in erythroblasts from day 0 to 9; Fig. 4A–D). A total of 17.3% of circRNA did not alter in expression between CD42− and CD42+ MK (Fig. 4D, group 5), and 17.7% of circRNA followed mRNA expression changes (groups 1 and 4). Conversely, in more than half of the circRNAs (65.1%), circRNA levels increased but the mRNA decreased (Fig. 4D; group 2; 14.5%) or remained unchanged (Fig. 4D; group 3; 50.5%). We found no circRNA with decreased expression levels and increased mRNA levels (Fig. 4D, group 6). In conclusion, the expression pattern of circRNA expression only partially follows the mRNA expression, and more than half of the circRNAs change their expression pattern independently of mRNA expression during erythroid and megakaryoid differentiation.

The majority of circRNAs expressed in differentiated cells correlates with that of mRNA expression in progenitors

Previous studies reported that circRNAs accumulate in neuronal and muscle cells upon differentiation (Westholm et al. 2014; Legnini et al. 2017; Kristensen et al. 2018). To test whether this accumulation is also seen during blood cell differentiation, we first compared the number of circRNAs identified in in vitro differentiated erythroblasts (Fig. 2D) with that of our previously published data on mature blood-derived RBC (Nicolet et al. 2018). The overlap of circRNA expression of in vitro differentiated RBC with mature RBCs was only 11.5% (676 out of 5878 high-confidence circRNAs; Fig. 4E, left panel). The overlap between circRNA expression in platelets (Nicolet et al. 2018) and MK (Supplemental Fig. S2F) was higher with 17.8% (1907 out of 10,729 high-confidence circRNA; Fig. 4E, right panel). This limited overlap could stem from the described uptake of transcripts by platelets from exogenous sources (Best et al. 2015) and could possibly include circRNAs. Alternatively, the differential circRNA expression could derive from transcription detected in progenitor

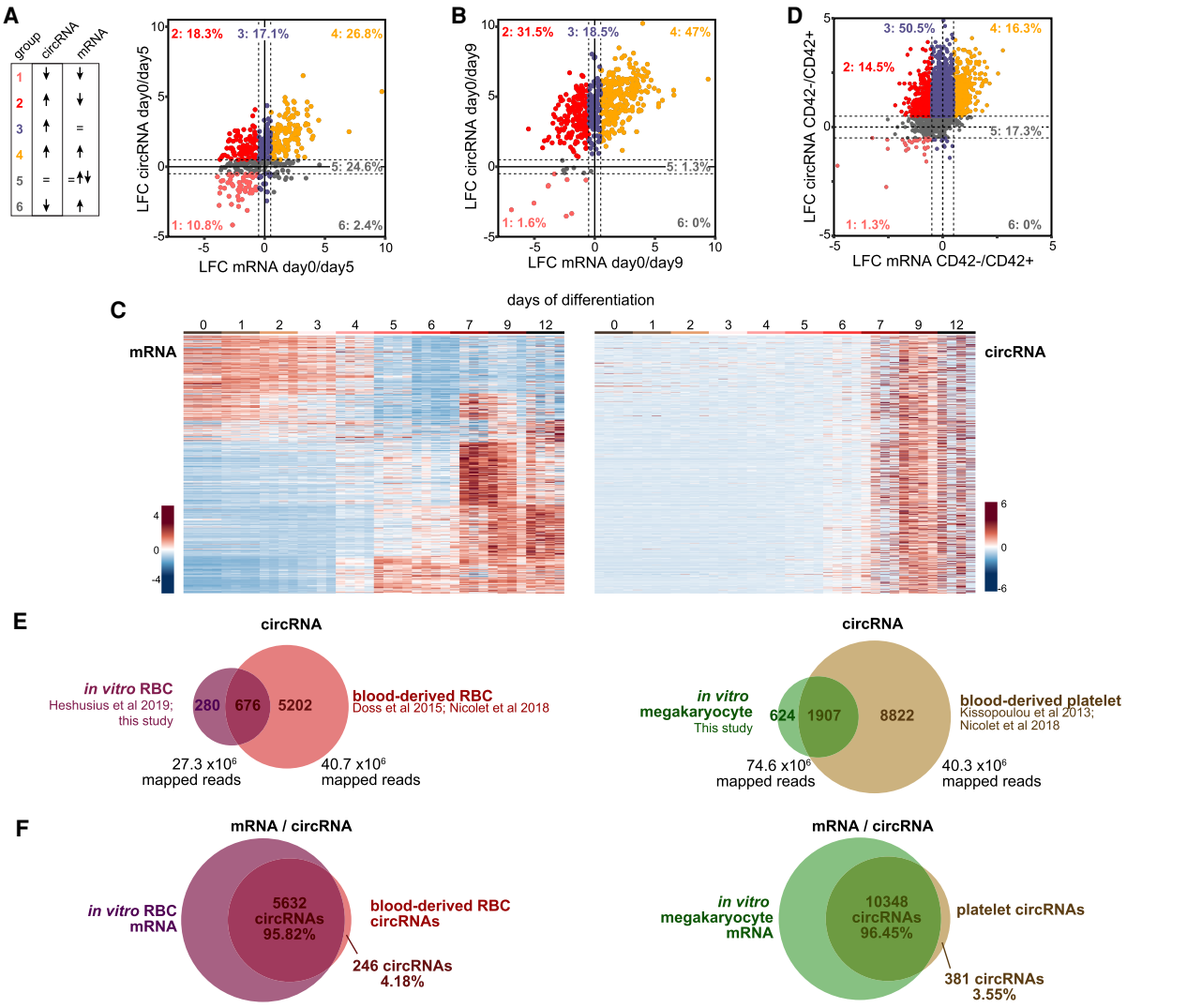

FIGURE 4. CircRNA expression can be independent of mRNA expression. (*A*,*B*) Log_2 fold change (LFC) for circRNA and corresponding mRNA was calculated for (*A*) day 0 to 5 and (*B*) day 0 to 9 of erythroid differentiation. CircRNA–mRNA pairs are represented in: decreased circRNA/decreased mRNA (group 1, pink), increased circRNA/decreased mRNA (group 2, red), increased circRNA/equal mRNA (group 3, purple), increased circRNA/increased mRNA (group 4, orange), equal circRNA (group 5, gray), decreased circRNA/increased mRNA (group 6, gray). (*C*) Heatmap of mRNA expression and matched circRNA expression for all high-confidence circRNA ($n = 950$, *Z*-score of reads per million mapped reads). Note that mRNA expression was detected using DCC at the circRNA position (see Materials and Methods). (*D*) LFC in circRNA and corresponding mRNA expression was calculated CD42– to CD42+ megakaryocytes differentiation. (*E*) Overlap in circRNA expression between in vitro RBC and ex vivo RBC (data from Doss et al. 2015; Nicolet et al. 2018; Heshusius et al. 2019; *left* panel; Fig. 1), and in vitro megakaryocytes and ex vivo platelets (Kissopoulou et al. 2013; Nicolet et al. 2018; *right* panel). Average sequencing depth is indicated *under* each population. (*F*) Overlap between circRNA in differentiated cells and mRNA in progenitor cells, for erythroid (*left* panel), and megakaryoid cells (*right* panel).

cells. To address the latter possibility, we compared the mRNAs expressed (full mRNA reads) by differentiating erythrocytes and megakaryocytes with that of circRNAs expressed RBCs and platelets, respectively. To our surprise, the mRNA-expressing genes of in vitro differentiating cells and circRNA-expressing genes of mature cells almost completely overlapped (95.82% and 96.45% for RBC and platelets, respectively, Fig. 4F). Thus, the circRNAs detected in enucleated platelets or RBCs correlate better with the mRNA expression than with that of circRNA expression in their respective progenitors. Thus, the discrepancy of circRNA expression between progenitors and mature cells reveals that the diversity of circRNA found in mature cells is not yet present in progenitor cells.

CircRNA expression does not correlate with changes in translation efficiency of the mRNA counterpart

A recent study showed that the YAP circRNA prevents the translation of its mRNA counterpart in a sequence-specific manner (Wu et al. 2019). Specifically, over-expression of YAP circRNA prevented the translation initiation complex

from engaging with the YAP mRNA (Wu et al. 2019). This finding prompted us to determine the transcriptome-wide correlation of endogenous circRNA expression with the translation efficiency of their mRNA counterpart. We used normalized expression data from the matched RNA-seq and Ribo-seq analysis of CD42− and CD42+ MKs (Supplemental Table S4). The ribosome footprint (RFP) reads fulfilled all quality controls upon mapping the reads onto the genome, that is, the read size distribution, periodicity, and reads distribution after P-site correction (Supplemental Fig. S3). We determined whether mRNA expression related to changes in RFP abundance by computing the LFC in mRNA abundance and the LFC in RFP abundance for each gene, between CD42− and CD42+ MK (Fig. 5A; Supplemental Table S4). Most changes in mRNA expression correlated well with changes in RFP counts (Pearson's correlation coefficient: 0.854). In addition, genes that expressed circRNAs (red dot) or not (gray dots) showed very similar patterns (Pearson's correlation coefficient: 0.768). This finding suggests that the ribosomal occupancy of mRNAs was not influenced by the coexpression of circRNA variants. Similarly, when we calculated the translation efficiency per gene *(normalized RFP counts [TPM]/normalized mRNA-seq [TPM])* (Fig. 5B), no differences in mRNA translation were observed between genes that do (red dots) or do not (gray dots) express circRNAs. Notably, 1942 mRNA-expressing genes (5.49%) altered their translation efficiency with LFC > 2 between CD42− and CD42+ MKs, while only 4 out of 1544 mRNA-expressing genes that also expressed circRNA (0.25%) displayed the same behavior (Fig. 5B; Supplemental Table S4).

We next determined whether changes in translation efficiency of mRNAs upon MK maturation related to the expression of circRNA from the same gene. Overall, we observed lower changes in translation efficiency in circRNA-expressing genes than circRNA-less mRNA-genes (span of LFC in translation efficiency = 5.42 and 29.55, respectively; Fig. 5B). This indicates that circRNA expression is associated with smaller changes in translation efficiency, suggesting a lack of effect on their mRNA counterpart. Indeed, only one circRNA (2.67%), *circ-UBAP2L*, altered its expression (LFC > 2) in CD42+ compared to CD42− MKs and showed an alteration in translation efficiency (LFC > 2) of the mRNA counterpart (Fig. 5C; blue dot). Closer examination of the mRNA, RFP, and circRNA levels of UBAP2L gene indeed suggested a correlation of changes in translation efficiency with circRNA expression (Fig. 5D).

To further examine whether the lack of abundant circRNA association with mRNA translation efficiency was specific to MKs or more broadly applicable, we examined the correlation of translation efficiency with circRNA expression throughout platelet maturation (Fig. 5E). We found that

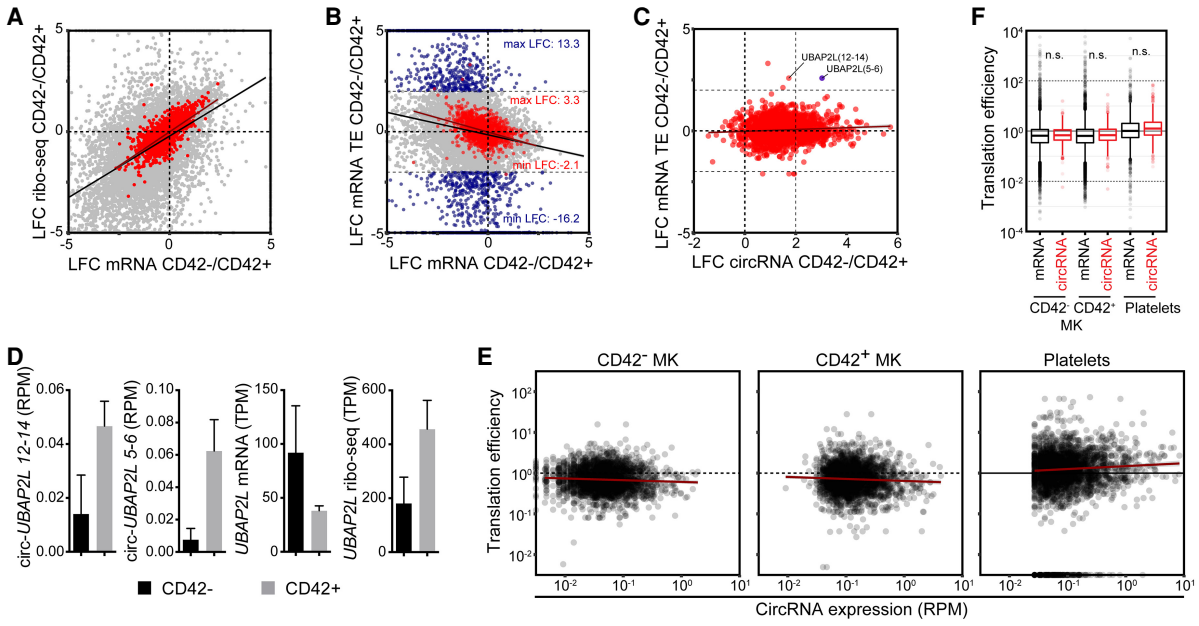

FIGURE 5. CircRNA-mediated regulation of mRNA translation is limited in megakaryocytes. (*A*) Log_2 fold change (LFC) in ribosomal occupancy (Ribo-seq) and mRNA expression between CD42− and CD42+ megakaryocytes. CircRNA-expressing genes are plotted in red. (*B*) LFC in translation efficiency (TE; see Materials and Methods) and mRNA expression between CD42− and CD42+ megakaryocytes. (*C*) LFC of translation efficiency and circRNA expression between CD42− and CD42+ megakaryocytes. Genes are plotted in blue in *B* and *C* when LFC in translation efficiency was more than fourfold (LFC > 2). (*D*) CircRNA, mRNA, and Ribo-seq expression of *UBAP2L*. (*E*,*F*) Relation between circRNA expression and translation efficiency (*E*) and translation efficiency for circRNA- and mRNA-only expressing genes (*F*) in CD42−, CD42+, and platelets. (*A*–*C*) The linear regression of all genes is represented in black, and this of circRNA expressing gene in dark-red. (RPM) reads per million mapped (linear) reads, (TPM) transcripts per kilobase per million.

the translation efficiency in CD42−, CD42+, and platelets remained uncorrelated to circRNA expression. Furthermore, the overall mRNA translation efficiency remained unchanged, whether the genes expressed circRNAs or not (Fig. 5F). Notably, this lack of association between circRNA and changes in translation efficiency of the mRNA counterpart was also observed in K562 and HeLa-S3 human cell lines (Supplemental Fig. S4). Combined, these findings indicate very limited effects of circRNAs on the translation efficiency of their mRNA counterpart.

CircRNAs contain putative open reading frames

Most circRNAs (~80%) are reported to fall in the coding region and/or contain the canonical translation start site (Memczak et al. 2013; Stagsted et al. 2019). We therefore sought to define the coding potential of megakaryocytic circRNAs. We used open reading frame (ORF)-finder (NCBI) to predict ORFs in high-confidence circRNAs. Because algorithms such as ORF-finder cannot mimic back-splicing in silico, we juxtaposed the circRNA sequence three times (termed 3xCircRNA; Supplemental Fig. S5A). This 3xCircRNA sequence allows the investigation of ORFs spanning over the back-splicing junction that could gain a stop codon as a result of frameshifts at the circRNA back-splicing junction. To identify ORFs that are common to both mRNAs and circRNAs, we also used the high-confidence circRNA sequence opened-up at the back-spliced junction (1xLinRNA; Supplemental Fig. S5A). Open reading frames with a minimal length of 25 aa and a canonical AUG start codon in the 1xLinRNA and the 3xCircRNA sequences were included in the analysis.

The majority of 1xLinRNA sequences (2371 out of the 2531) in MKs contained putative ORFs ($n = 8519$ unique ORFs; mean ORF length: 77.3 aa; median: 46 aa). Similarly, 2488 out of 2531 3xCircRNA contained at least one predicted ORF ($n = 12{,}567$ unique ORFs; mean ORF length: 115.9 aa; median: 55 aa; Fig. 6A). To isolate circRNA-specific ORFs, we subtracted the ORFs found in 1xLinRNA from those found in 3xCircRNA sequences. Whereas 7559 unique ORFs were shared by both sequences (mean ORF length: 66.99 aa; median: 42 aa), 5008 unique ORFs were specific for 2428 circRNAs (mean ORF length: 189.6 aa; median: 109 aa; Fig. 6B). Thus, 95.93% of circRNAs in MKs have specific putative open reading frames. CircRNA-specific putative ORFs were also detected in platelets, with 19,995 ORFs (6904 out of 10,729 circRNAs, 64.3% of circRNA), and in differentiating erythroblasts, with 1864 ORFs (639 out of 950 circRNAs, 67.3% of circRNA; Supplemental Fig. S5B,C).

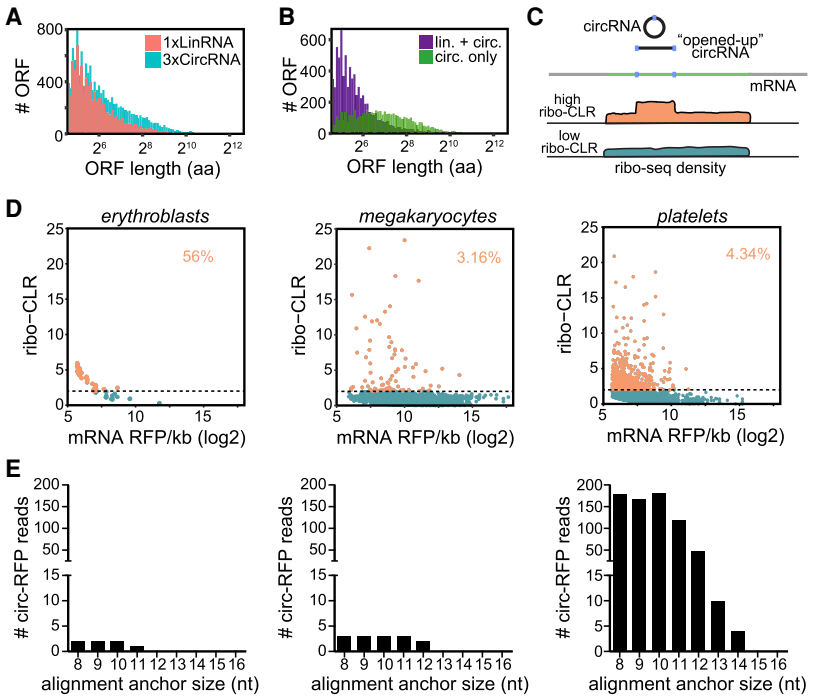

FIGURE 6. Putative ORF detection in circRNAs, with limited evidence for translation. (*A*) Open reading frames (ORFs) were computed (see Materials and Methods) for linearized high-confidence circRNA sequences (1xLinRNA), and for tripled juxtaposed linearized sequence of high-confidence circRNA in megakaryocytes to include circularized junction areas (3xCircRNA, see Supplemental Fig. S4A). Bar graph depicts the length and frequency of all identified ORFs found in 1xLinRNA (pink) or 3xCircRNA (blue). (*B*) Bar graph depicting the length and frequency of the ORFs found in both 1xLinRNA and 3xCircRNA sequences (purple) or specifically in circRNA (green). (*C*,*D*) Ribosome-footprinting sequencing (Ribo-seq) data were used to determine the ribosome density per kilobase on mRNA sequence and circRNA sequence. The circular-over-linear ribosome density ratio (RiboCLR) was calculated. (*C*) Schematic representation of circRNA (back-spliced junction in blue) and mRNA sequence, and Ribo-seq density resulting in high or low Ribo-CLR. (*D*) Calculated Ribo-CLR for erythroblasts (*left* panel), megakaryocytes (*middle* panel), and platelets (*right* panel) and plotted against the mRNA ribosome footprint (RFP) density (RFP per kilobase). (*E*) Ribo-seq data of erythroblasts (*left* panel; data from Mills et al. 2016), CD42− or CD42+ megakaryocytes (*middle* panel), and platelets (*middle* panel; data from Mills et al. 2016) were screened for RFP reads on the circRNA junction (circ-RFP) using CE2. The minimum chimeric alignment anchor size for alignment (8–16 nt) is indicated. Circ-RFP that were not found expressed in low-confidence circRNA (based on RNA-seq detection) were excluded.

A subset of circRNAs displays a high ribosome density

To determine whether the circRNA-containing putative ORFs show any evidence of translation into proteins, we re-analyzed previously published RFP sequencing data from

erythroblasts (Mills et al. 2016). We determined the ribosome density on the coding region of mRNA sequence, and on the circRNA sequence (Fig. 6C). We mapped the RFP read on the whole mRNA coding sequence and on the "high-confidence" circRNA sequence that was opened-up at the back-spliced junction. We then calculated the RFP density per kilobase on the mRNA and the circRNA sequences. To measure differences in RPF reads between circRNA and mRNA, we calculated the ratio of circRNA-over-mRNA RFP reads density (Ribo-CLR). Of note, a Ribo-CLR > 1 would be indicative of a higher RFP density over the circRNA sequence than on the mRNA sequence. Erythroblasts contained only 57 circRNA–mRNA Ribo-seq pairs that had reliable expression levels (>50 RFP per kilobase; Fig. 6D, left panel; Supplemental Table S4). Of these 57 circRNAs, 32 (56% of pairs) had a Ribo-CLR > 2. It is thus conceivable that these 32 circRNAs are translated in erythroblasts.

In MK Ribo-seq data, the vast majority (96.84%) of the circRNA-expressing genes had a Ribo-CLR below two, which indicates similar mRNA and circRNA RFP read densities (Fig. 6D, middle panel; Supplemental Table S4). Indeed, of the 2531 circRNAs, only 80 (3.16%) showed a higher RFP density than their corresponding mRNA (Supplemental Table S4). Lastly, we reanalyzed published Ribo-seq data of platelets (Mills et al. 2016). Four hundred and sixty-five circRNAs showed a Ribo-CLR > 2 (Fig. 6D, right panel; Supplemental Table S4). Nevertheless, with 4.34% of all 10,729 circRNAs, the overall percentage of circRNAs that could potentially contribute to the platelet proteome resembled that of MK. Of note, due to the natural 5′ bias of Ribo-seq data (Supplemental Fig. S3B) we observed that circRNAs starting at exons closer to the 5′ of the CDS tended to have Ribo-CLR > 2 (Wilcoxon signed rank test; $P = 9.098 \times 10^{-05}$; Supplemental Fig. S5D). Thus, a small proportion of circRNAs in erythrocytes, megakaryocytes, and platelets showed a higher ribosome density than their mRNA counterpart.

CircRNAs in platelets show hundreds of ribosome footprints on the back-spliced junction

Ribosome occupancy should also be found at the back-spliced junction of the circRNA, if this region contributes to the putative circRNA-specific coding region. We therefore re-screened all RFP reads from erythrocytes, megakaryocytes, and platelets and with an adaptation of the Ribo-seq reads alignment to allow for chimeric reads detection and subsequent back-spliced junction detection. Overlap of the chimeric reads to the genome was set with a minimum anchor point of 8 to 16 nt on either side of the read. We also allowed one mismatch. Of the 114 million reads in erythroblasts, we found only two RFP reads for anchors of 8, 9, or 10 nt (Fig. 6E, left panel; Supplemental Table S4). The two RFPs corresponded to two circRNAs *circ-ARHGEF12* and *circ-SPECC1*. As the median Ribo-seq read density in erythroblasts reached 1.984×10^{-3} reads per nt, one would already expect by chance about 53 reads on the 950 "high-confidence" circRNA (0.055 read/circRNA junction).

We also screened the 757 million Ribo-seq reads in megakaryocytes for ribosome footprints at the back-spliced junction. As the median Ribo-seq read density for all translated genes in megakaryocytes was 0.105 reads per nt, one would expect by chance about 7428 reads on the 2531 "high-confidence" circRNA if they were translated (2.93 reads/circRNA junction). However, only three RFPs reads matching circRNAs in megakaryocytes were detected (Fig. 6E, middle panel; Supplemental Table S4). These three RFPs reads corresponded to two circRNAs; that is, *circ-PRDM2* and *circ-YEATS2*.

Of the ∼178 million RFP reads in platelets, one would expect by chance about 3378 RFPs on the 10,729 "high-confidence" circRNA of platelets (median RFP density on mRNA 0.011 read/nucleotide, 0.314 read/circRNA junction). Yet, we only detected 180 RFPs, 168 RFPs, and 182 RFPs over the circRNA back-spliced junction in platelets with an anchor size of 8, 9, and 10 nt, respectively (Fig. 6E, right panel; Supplemental Table S4). The circRNA-RFPs corresponded to 56 different circRNAs. Of note, 13 of these 56 circRNAs (*HIPK3, TMEM135, CORO1C, DNAJC6, GSAP, ASH2L, FAM120A, MCU, FARSA, WDR78, ZC3H6, NCOA2, APOOL*) also displayed a Ribo-CLR > 2 (Supplemental Fig. S5E), indicating ribosome reads on both the back-spliced junction and the full circRNA sequence. Overall, the RFP analysis showed some but limited evidence of translation, in particular in MK, and erythroblasts. Of note, the low numbers of RFP on the circRNA junction did not allow us to perform a reliable periodicity analysis. Together, platelets provide the best indication of putative circRNA translation, with—based on the sequencing depth of the Ribo-seq data sets—approximately 58 times more circRNA-specific Ribo-seq reads than erythroblast and approximately 258 times more than megakaryocytes.

Mass spectrometry fails to identify circRNA-specific peptides in platelets

Because the RFP analysis in platelets showed the highest probability of translation, we further searched for evidence of translation in this cell type. We generated a reference peptide library from the three translation frames over the 508 circRNA back-spliced junction of the high-confidence circRNAs with Ribo-CLR above two or detected circ-RFP. Translation frame(s) that contained a STOP codon before the back-spliced junction were excluded from this reference peptide library. This left 1566 unique putative circRNA peptides spanning the back-spliced junction with a minimum of five amino acids overhang. Of these 1566 putative circRNA peptides, 12 (0.77%) did not contain

lysine nor arginine, 97 (6.2%) and 123 (7.9%) contained only arginine, or lysine, respectively. Thereby the majority (99.2%) of putative circRNA peptides are cleavable by trypsin treatment and should be detectable by mass spectrometry. To also identify circRNA-specific peptides outside the circRNA-junction, we included the full-length circRNA-specific putative ORFs of platelets in the peptide library we identified in Supplemental Figure S4B. Lastly, we also included the reference proteome (UniProt) as decoy, to prevent possible "background" hits to match known canonical protein sequences. Published MS data of platelets (Van Oorschot et al. 2019) were used to search for circRNA-specific peptides. Of the 192,743 identified peptides, not one peptide matched a circRNA junction (Supplemental Fig. S5E). Thus, even though Ribo-seq data suggest some possible translation from circRNAs in platelets, the detection of peptides from back-spliced circRNA junctions, or from circRNA-specific ORFs fall—if present at all—below the detection limit of data-dependent mass spectrometry analysis.

DISCUSSION

In this study, we present a comprehensive analysis of circRNAs in terminal differentiation of erythroblasts and platelets. CircRNA expression is in particular increased at enucleation in erythroid differentiation. This could reflect an accumulation of transcript degradation leftovers upon enucleation, as previously suggested (Alhasan et al. 2016). While this is an attractive hypothesis, not all circRNA follow this overall trend. In fact, more than 50% of circRNAs were regulated independently from changes in linear mRNA expression. This was true when we compared differences in expression levels prior to and post-enucleation. We also observed a clear increase in number and expression levels of specific circRNAs at enucleation, which were not detected in progenitors. This increase of circRNA number and amount is unlikely to stem from a technical reason, as all samples had sufficient sequencing depth (~30 million reads) to allow for a reliable detection of lowly expressed circRNA. Thus, the majority of measured circRNAs in terminally differentiated erythrocytes cannot be explained by mere accumulation from progenitors alone. This was also true for circRNA expression in MK compared to platelets. Future studies could use metabolic labeling such as 4-thiouridine (4sU) to investigate the de novo circRNA expression in relation to their mRNA counterparts.

Another possible explanation for the increase in circRNA during erythroid maturation could be the loss of the circRNA degradation machinery. Even though it is not fully understood how circRNAs are degraded, the RNase-L, G3BP1, and G3BP2 have been implicated in this process (Liu et al. 2019; Fischer et al. 2020). Notably, G3BP1 and 2 are down regulated during erythroid maturation, and RNase-L is absent in mature erythrocytes (Gautier et al. 2016). It is therefore tempting to speculate that the loss of the circRNA degradation machinery in mature erythrocytes contributes to the increased circRNA levels.

Intriguingly, the circRNAs in differentiated RBCs and platelets strongly overlapped with the mRNAs that were expressed in their progenitors. It has been proposed that splicing occurs in the cytoplasm of platelets and MK (Denis et al. 2005; Nassa et al. 2018). It is therefore tempting to speculate that back-splicing and formation of circRNA could also occur in the cytoplasm. In line with this, several splicing factors were detected in platelets by MS analysis (Burkhart et al. 2012; Van Oorschot et al. 2019), including DHX9. Therefore, at the period of enucleation of erythrocytes and during platelet formation, mRNA could be circularized, and thus contribute to increased numbers of circRNAs during enucleation and therefore explain the substantial overlap with the mRNAs in progenitors. This hypothesis, however, requires experimental confirmation. In addition, MK can sort specific mRNA into platelets (Cecchetti et al. 2011). Whether circRNA can also be sorted and whether this sorting could explain some of the discrepancy between MK and platelets circRNA content, is yet to be uncovered.

About 4% of circRNAs in platelets and erythrocytes did not overlap with the mRNA levels in MK and differentiating erythroblasts. These circRNAs could be acquired from other cell types in the circulation, as observed for linear RNA in the context of tumor "educated" platelets (Best et al. 2015), or endogenous vascular-derived RNA (Clancy et al. 2017). A study in platelets from healthy and diseased individuals could shed light on this. If true, circRNAs taken up by platelets or erythrocytes could in fact serve as novel biomarkers, which could be in particular valuable for diagnostics due to their high stability.

The function of circRNAs still remains elusive. CircRNA could serve to reinforce transcription, and lead to differential exon usage as previously proposed (Kelly et al. 2015). Differential exon usage was also recently reported to be supported by pre-mRNA exonic sequences (Fiszbein et al. 2019). Whether this is indeed occurring in primary blood cells is yet to be determined.

CircRNAs are also reported to regulate mRNA translation in a sequence-specific manner (Sun et al. 2019; Wu et al. 2019; Li et al. 2020). We investigated here the possible effect of circRNA on its mRNA counterpart. We only identified one circRNA in MKs that show limited indications for translation regulation. In addition, we found no correlation between translation efficiency of mRNA and the expression level of their circular counterpart, whether in MK, platelets, or human cell lines. Whether our findings in MKs are also applicable to enucleated erythrocytes is not known. CircRNA-mediated regulation of mRNA translation is an attractive hypothesis in erythrocytes, because

the majority of translation is shut down in mature cells (Mills et al. 2016), and circRNAs could support translation shutdown. In addition, it is also conceivable that circRNA affect translation of other mRNA (Sun et al. 2019; Li et al. 2020).

CircRNAs were also shown to be translated (Legnini et al. 2017; Pamudurti et al. 2017; Yang et al. 2017; Liang et al. 2019; Huang et al. 2021), in particular from exogenously expressed circRNAs. This finding suggests that the highly stable circRNA transcripts could help maintain the proteome in long-lived red blood cells and platelets. However, we found very limited indications that translation from endogenous circRNAs occurs. Similar to a recent study (Stagsted et al. 2019), we detected only a few circRNA-specific RFP. The low number of detected circRNA-specific RFP reads could not be explained by low sequencing depth, as the Ribo-seq data sets entailed 114, 757, 178 million reads in erythroblasts, MKs, and platelets, respectively. Yet, only platelets had 180 RFP reads on the circRNA back-spliced junction. Nevertheless, whether the increase of circRNA-specific RFP stems from active translation or from the loss of regulators of ribosome homeostasis such as PELO by erythrocytes and platelets (Mills et al. 2016) is yet to be determined.

Deep MS analysis on platelets did not identify peptides from circRNA back-spliced junctions. Yet, circRNA-derived proteins may be generated on low levels and/or result in production that is below the detection limit of MS. This finding is corroborated by recent ribosome-footprint analysis that found very limited translation of >300.000 circRNAs (0.73% of circRNAs), and closely matches our findings (0.52%; 56 out of 10,729 circRNAs in platelets [Huang et al. 2021]). Indeed, as circRNA peptides are only found in minute abundance, their detection was shown to be indistinguishable from noise in MS data (Hansen 2021). Nonetheless, immunoprecipitation enrichment of specific targets could help to overcome this detection limit for specific circRNA (Pamudurti et al. 2017; Liang et al. 2019).

mRNA translation also may mask the circRNA translation and its contribution to the proteome, when the circRNA-derived peptides are identical to the mRNA-derived peptides. Nevertheless, because only 117 out of the 465 circRNAs (25.16%) with high Ribo-CLR show protein expression in MS, the relative contribution of circRNA-derived translation is arguably limited in light of the mRNA-derived translatome. Compiled, our study thus only supports a limited possible contribution of circRNA-translation to the proteome in platelets.

In conclusion, we provide here the landscape of circRNA expression during erythroid differentiation and megakaryocyte maturation. This study can serve as a blueprint for future studies in these cell types. Our results also challenge the current views on the ubiquitous functions proposed for circRNAs in the biological context of terminal hematopoiesis.

MATERIALS AND METHODS

CircRNA identification and analysis

Data on erythroblast differentiation were retrieved from our previous study (Heshusius et al. 2019). circRNA identification was performed with the previously established circRNA detection pipeline (Nicolet et al. 2018). Briefly, the quality of RNA-seq reads was assessed using FastQC version 0.11.8 (Simon Andrews, Babraham Institute). Data were aligned to the human genome (GRCh37/hg19-release75) using STAR version 2.5.2b (Dobin and Gingeras 2015) allowing for chimeric detection, with an overhang "anchor" of 15 nt on either side of the read. The chimeric output file of STAR was analyzed with DCC 0.4.6 (Cheng et al. 2015) and CircExplorer2 (CE2) 2.3.2 (Zhang et al. 2014) to detect, filter, and annotate circRNA. DCC was used for detection of linear reads at the circRNA coordinates (using the option-G). CircRNA expression was considered low confidence when at least two junction reads were found in at least one sample by both DCC and CE, and high confidence detection when at least two junction reads were found in all biological replicates of one specific cell type, by both tools. Supporting circRNA read counts were normalized to reads per million mapped reads (RPM). The maximal circRNA spliced length was calculated with the exon length information provided by the CE2 annotations. These annotations were then used to calculate the first and last circularized exon. For differential expression analysis of high-confidence circRNA, we used DESeq2 (Love et al. 2014) with *P*-adjusted <0.05. We used the total number of mapped reads per sample to calculate the scaling factors, instead of the automatic scaling factors detection of DESeq2. The LFC was calculated using the formula:

$$\mathrm{LFC(AB)} = \log_2(\mathrm{B}) - \log_2(\mathrm{A}).$$

Data analysis was performed in R (3.5.1) and R-Studio (1.1.453).

RNA-seq analysis of mRNA and ncRNA

After quality control with FastQC, raw RNA-seq reads were aligned with Salmon version 0.13.1 (Patro et al. 2017) on the coding and noncoding transcriptome (ENSEMBL, GRCh38 release 92) to obtain TPM normalized counts. To get mRNA and ncRNA expression per gene, TPM counts were summed up per gene name, according to ENSEMBL BioMart annotations (Kinsella et al. 2011). Clustering of blood cells based on mRNA expression was performed using *hclust()* and *prcomp()*.

In vitro megakaryocyte differentiation

Megakaryocytes were cultured from human cord blood-derived CD34+ cells. Cord blood cells were obtained after informed consent and with the approval of the ethical committee of local hospitals. Cord blood was diluted in PBS, loaded on ficoll-pague (GE Healthcare), and centrifuged 15 min at 400*g*. The white blood cell layer was collected from the ficoll gradient, washed twice in PBS + 1 mM EDTA + 0.2% HSA. CD34+ cells were purified with anti-CD34 Microbeads (Miltenyi Biotec 130-046-702) and MACS LS column (Miltenyi, 130-042-401) according to manufacturer's guidelines. Purity for CD34+ cells was >90%, as determined by flow-cytometry with anti-CD34 antibody (#581-PE; Beckman Coulter,

measured on Beckman Coulter FC500). CD34+ cells were seeded at a density of 50.000 cells/well in a 12-well plate in CellgroSGM (CellGenix) supplemented with 100 ng/mL human recombinant TPO (CellGenix, Cat.1417) and 10 ng/mL IL1β (Miltenyi Biotec, Cat.130-093-895). At day 3, 1:1 fresh media was added with an additional 10 ng/mL TPO and 1 ng/mL IL1β. On day 5, cells were split at a density of 100.000 cells in six-well plates, and fresh media with 10 ng/mL TPO and 1 ng/mL IL1β was added. On day 10, cells were harvested and supplemented with 100 µg/mL Cycloheximide (Sigma, Cat. 1810-1G) in culture medium prior to cell sorting.

Megakaryocyte selection

Cultured cells were harvested when >85% of cells were CD41a+ (CD41a-APC; clone HIP8; BD Pharmingen; Cat. 559777), as determined by flow-cytometry. Cells were pelleted at 120*g* for 1 min at 4°C and washed once in ice cold buffer (PBS, 1 mM EDTA, 0.2% HSA + 100 µg/mL cycloheximide). Two-step selection was performed on ice with the EasySep Human PE-Positive Selection Kit (18551), using anti-human CD42b-PE (clone HIP1, BD Pharmingen, 555473) according to manufacturer's guidelines. CD41a+ CD42b− and CD41a+ CD42b+ cell fractions were selected, washed using PBS + 100 µg/mL cycloheximide, and kept on ice until further processing. Viability of the cells was >90% (7-AAD, BioLegend), and purity for CD41a+ CD42b− was >85% and CD41a+ CD42b+ was >95%, as determined by flow-cytometry. Cells were immediately processed.

RNA sequencing

Cell lysis and RNA isolation for RNA sequencing and ribosomal footprinting were performed according to Ingolia et al. (2009) with some adaptations. Briefly, CD42− and CD42+ selected megakaryocytes were pelleted. Cell pellets were dissolved in 150 µL ice cold lysis buffer (20 mM Tris pH 7.4, 250 mM $NaCl_2$, 5 mM $MgCl_2$, 0.5% Triton X-100, 1 mM Dithiotreitol (DTT), 0.024 U/µL Turbo DNase (Ambion), 0.01 U/µL RNaseOUT (Invitrogen), and 100 µg/mL Cycloheximide). The lysate was immediately split in two aliquots of 50 and 100 µL, for total RNA sequencing and ribosomal footprint analysis, respectively. An amount of 2.5 µL SUPERase In RNase Inhibitor (Invitrogen) was immediately added to the total RNA sample, and total RNA was extracted using the miRNeasy Kit (Qiagen) according to manufacturer's protocol. RNA quality was assessed on Agilent bioanalyzer RNA chip (all samples with RIN > 9.0), and quantified using Qubit 2.0 (Thermo Fisher). Ribosomal RNA was removed using Ribo Zero Gold (Epicentre/Illumina; 20020596) using the manufacturer's protocol, and the cDNA library was constructed with the KAPA Stranded RNA-Seq Kit (KAPA Biosystems KK8400) according to manufacturer's protocol with Illumina TruSeq forked adapters. Library quality was assessed on an Agilent Bioanalyzer high sensitivity DNA chip and quantified using qPCR with the KAPA Library Quantification Kit (KK4824). Libraries were pooled to a 2 nM concentration and 125 bp paired-end reads were sequenced on HiSeq 2000 (Illumina).

Ribosomal footprinting

An amount of 100 µL of cell-lysates was used for ribosome footprinting preparation. Samples were kept on ice for 10 min and regularly vortexed to fully lyse the outer membranes and release the ribosomes. Lysates were spun at 20,000*g* for 10 min at 4°C and supernatant was harvested to remove the remaining pelleted cell debris and nuclei. Lysates were treated with 2 µL of RNase 1 (Ambion) and incubated at 37°C for 45 min. The reaction was stopped by the addition of 5 µL SUPERase In RNase Inhibitor. Lysates were loaded on a 1-M 0.150 mL Sucrose cushion in 8 × 34 mm polycarbonate thick wall tubes and centrifuged at 120,000*g* for 30 min in a TLA-120.1 rotor in a precooled 4°C tabletop ultracentrifuge. The pellet was resuspended using 100 µL resuspension buffer (10 mM Tris pH 7.0, 1% SDS and 0.01 U/µL proteinase K [NEB]) for 30 min at 37°C. Footprints were subsequently extracted with the miRNeasy Kit according to manufacturer's guidelines for small RNA. rRNA contamination was removed using the Ribo-Zero Gold rRNA Removal Kit (Epicentre/Illumina; 20020596). Footprint RNA quality was assessed using the Agilent Bioanalyzer using the RNA chip. Footprints were selected for 26–34 nt with custom markers (see Ingolia et al. 2009) on the Elchrom Scientific ORIGINS system and short fragment gels, using gel electro-elution into Spectra/Por 3 3.5KD MWCO dialysis membranes. Libraries were produced using the Art-Seq Kit (Epicentre/Illumina) according to the manufacturer's protocol. The quality of libraries was assessed on an Agilent Bioanalyzer with a high sensitivity DNA chip and quantified using qPCR with the KAPA Library Quantification Kit (KK4824). Libraries were pooled to a 2 nM concentration and sequenced on HiSeq 2000 (Illumina).

Ribo-seq analysis

The quality of raw Ribo-seq reads was assessed using FastQC. Reads were trimmed for sequencing adapters using Trimmomatic version 0.39 (Bolger et al. 2014) or cutadapt version 3.0 (Martin 2011), excluding reads <25 and >35 nt long. Additional quality control was performed on the BAM files resulting from genome mapping with STAR in Ribo-seQC (Calviello et al. 2019).

Trimmed reads were mapped with Salmon on the human transcriptome (GRCh38 release 92) to get TPM normalized counts. Using a k-mer of 11 performed best for Ribo-seq mapping to build the Salmon index. Translation efficiency was obtained by dividing the normalized Ribo-seq counts in TPM by the normalized RNA-seq counts in TPM. To estimate the ribosome footprint read density, we used the linearized sequence of high-confidence circRNA and the coding transcriptome. After aligning the Ribo-seq reads with Salmon, Ribo-seq reads density per kilobase were obtained by dividing the estimated counts (not TPM) by circRNA length (for circRNA) and CDS length (for mRNA). The circular-over-linear Ribo-seq reads density per kilobase (Ribo-CLR) was obtained by dividing the circRNA Ribo-seq density per kilobase, by the Ribo-seq density per kilobase of mRNA. The ratio was calculated separately for each sample and averaged per population. Ribo-seq data for erythroblast and platelets were retrieved from a previous study (Mills et al. 2016).

CircRNA-specific detection from Ribo-seq reads

To identify circRNA-specific Ribo-seq reads, we used an approach similar to the "classical" circRNA detection described above. Genome alignment as described above with STAR was used for chimeric reads detection with incremental anchors of 8–16 nt

on either side of a chimeric read, allowing for one mismatch. CE2 was then used to detect, quantify, and annotate the circRNAs, and data were further processed in R.

ORF prediction

The linearized, spliced "high-confidence" circRNA sequences were obtained using BEDtools version 2.18 (Quinlan and Hall 2010). The sequence was juxtaposed three times to mimic a circRNA sequence. Open reading frames (ORFs) were predicted for both linearized circRNA sequence (1xLinRNA) and tripled (3xCircRNA) sequences using ORF-finder (version 0.4.3; NCBI). Resulting ORF sequences were analyzed and filtered in R.

Detection of circRNA peptides by mass spectrometry

The high-confidence circRNA sequences including all exons between first and last exon were obtained using BEDtools. The last 77 nt of the circRNA sequences were joined to the first 77 nt to generate a junction sequence library. This library was translated in three frames. Open reading frames (ORFs) that presented a length <30 amino acids (i.e., not spanning the circRNA junction) were removed. All ORFs were transformed into a fasta library. A proteome reference library containing circRNA junction ORFs, as well as circRNA-specific ORFs (from 3xCircRNA sequences of platelets, filtered for unique circ-specific ORFs), and Uniprot Human proteome reference (downloaded 13-02-2019), was constructed and used for peptide matching with Proteome Discoverer (version 2.2; Thermo Fisher) of our previously published mass spectrometry data set on platelets from healthy donors (Van Oorschot et al. 2019). The precursor mass tolerance was set to 10 ppm with a fragment mass tolerance of 0.6 KDa and a target FDR of 0.01. Only peptides with high confidence detection in MaxQuant were considered.

Plots and graphs

Heatmaps were generated in R using corrplot (Wei and Simko 2017) or pheatmap 1.0.8 (Kolde 2012). Plots and graphs were generated with ggplot2 (Wickham 2016) in R, or Graphpad PRISM version 7.0.

Data retrieval and deposition

For ex vivo RBC and platelet analysis, we used our previously published data sets. Data were retrieved from the National Center for Biotechnology Information (NCBI) Gene Expression Omnibus (GEO) and Sequence Repository Archive (SRA) accession numbers for platelets (project: PRJEB4522): ERR335311, ERR335312, and ERR335313 (Kissopoulou et al. 2013); for RBCs: (GEO: GSE63703) SRR2124299, SRR2124300, SRR2124301, and (GEO: GSE69192) SRR2038798 (Doss et al. 2015; Alhasan et al. 2016); for erythroid differentiation: GEO: GSE124363 (Heshusius et al. 2019); and for human cell lines GEO: GSE125218 (Martinez et al. 2020).

Ribosome-footprinting data sets of platelets and erythroblasts were retrieved from GEO with accession number: GSE85864 (Mills et al. 2016), and for those of human cell lines GEO: GSE125218 (Martinez et al. 2020). For comparison to the previous study of our transcriptome data, we retrieved additional data sets from HSC and MEP (Notta et al. 2016); cultured megakaryocytes (Bhatlekar et al. 2020); pro-, early/late basophilic, poly-, and ortho-chromatic erythroid cells (An et al. 2014).

Raw mass spectrometry data sets of platelets were obtained from the PRoteomics IDEntifications Database (PRIDE) repository under the accession number PXD009020 (Van Oorschot et al. 2019).

DATA DEPOSITION

Ribosome footprinting and an RNA-seq data set of megakaryocytes were deposited on NCBI's Gene Expression Omnibus (GEO) with accession number GSE159579. Scripts used in this study are accessible on GitHub (https://github.com/BenNicolet/CircRNA_in_MK_and_Erys).

SUPPLEMENTAL MATERIAL

Supplemental material is available for this article.

ACKNOWLEDGMENTS

This research was supported by the European Research Council (ERC, consolidator grant), by the Dutch Science Foundation (Apasia grant), and by Oncode (all to M.C.W.). We also thank S. Heshusius for helpful discussions, and M. Hansen, P.J. van Alphen, and M. van den Biggelaar for critical reading of the manuscript.

Author contributions: B.P.N. analyzed data; B.P.N., S.J., and E. H. performed experiments. M.C.W., W.H.O., E.v.d.A., and M.v.L. supervised; B.P.N. and M.C.W. wrote the manuscript.

Received March 17, 2021; accepted October 19, 2021.

REFERENCES

Aktaş T, Ilik IA, Maticzka D, Bhardwaj V, Pessoa Rodrigues C, Mittler G, Manke T, Backofen R, Akhtar A. 2017. DHX9 suppresses RNA processing defects originating from the Alu invasion of the human genome. *Nature* **544:** 115–119. doi:10.1038/nature21715

Alhasan AA, Izuogu OG, Al-Balool HH, Steyn JS, Evans A, Colzani M, Ghevaert C, Mountford JC, Marenah L, Elliott DJ, et al. 2016. Circular RNA enrichment in platelets is a signature of transcriptome degradation. *Blood* **127:** e1–e11. doi:10.1182/blood-2015-06-649434

An X, Schulz VP, Li J, Wu K, Liu J, Xue F, Hu J, Mohandas N, Gallagher PG. 2014. Global transcriptome analyses of human and murine terminal erythroid differentiation. *Blood* **123:** 3466–3477. doi:10.1182/blood-2014-01-548305

Ashwal-Fluss R, Meyer M, Pamudurti NR, Ivanov A, Bartok O, Hanan M, Evantal N, Memczak S, Rajewsky N, Kadener S. 2014. CircRNA biogenesis competes with pre-mRNA splicing. *Mol Cell* **56:** 55–66. doi:10.1016/j.molcel.2014.08.019

Best MG, Sol N, Kooi I, Tannous J, Westerman BA, Rustenburg F, Schellen P, Verschueren H, Post E, Koster J, et al. 2015. RNA-seq of tumor-educated platelets enables blood-based pan-

cancer, multiclass, and molecular pathway cancer diagnostics. *Cancer Cell* **28:** 666–676. doi:10.1016/j.ccell.2015.09.018

Bhatlekar S, Manne BK, Basak I, Edelstein LC, Tugolukova E, Stoller ML, Cody MJ, Morley SC, Nagalla S, Weyrich AS, et al. 2020. miR-125a-5p regulates megakaryocyte proplatelet formation via the actin-bundling protein L-plastin. *Blood* **136:** 1760–1772. doi:10.1182/blood.2020005230

Bolger AM, Lohse M, Usadel B. 2014. Trimmomatic: a flexible trimmer for Illumina sequence data. *Bioinformatics* **30:** 2114–2120. doi:10.1093/bioinformatics/btu170

Burkhart JM, Vaudel M, Gambaryan S, Radau S, Walter U, Martens L, Geiger J, Sickmann A, Zahedi RP. 2012. The first comprehensive and quantitative analysis of human platelet protein composition allows the comparative analysis of structural and functional pathways. *Blood* **120:** 73–82. doi:10.1182/blood-2012-04-416594

Calviello L, Sydow D, Harnett D, Ohler U. 2019. Ribo-seQC: comprehensive analysis of cytoplasmic and organellar ribosome profiling data. bioRxiv doi:10.1101/601468v1

Cecchetti L, Tolley ND, Michetti N, Bury L, Weyrich AS, Gresele P. 2011. Megakaryocytes differentially sort mRNAs for matrix metalloproteinases and their inhibitors into platelets: a mechanism for regulating synthetic events. *Blood* **118:** 1903–1911. doi:10.1182/blood-2010-12-324517

Chen LL. 2016. The biogenesis and emerging roles of circular RNAs. *Nat Rev Mol Cell Biol* **17:** 205–211. doi:10.1038/nrm.2015.32

Cheng J, Metge F, Dieterich C. 2015. DCC – specific identification and quantification of circular RNAs from sequencing data. *Bioinformatics* **32:** 1–13.

Clancy L, Beaulieu LM, Tanriverdi K, Freedman JE. 2017. The role of RNA uptake in platelet heterogeneity. *Thromb Haemost* **117:** 948–961. doi:10.1160/TH16-11-0873

Denis MM, Tolley ND, Bunting M, Schwertz H, Jiang H, Lindemann S, Yost CC, Rubner FJ, Albertine KH, Swoboda KJ, et al. 2005. Escaping the nuclear confines: signal-dependent pre-mRNA splicing in anucleate platelets. *Cell* **122:** 379–391. doi:10.1016/j.cell.2005.06.015

Dobin A, Gingeras TR. 2015. Mapping RNA-seq reads with STAR. *Curr Protoc Bioinformatics* **51:** 1.14.1–11.14.19. doi:10.1002/0471250953.bi1114s51

Doss JF, Corcoran DL, Jima DD, Telen MJ, Dave SS, Chi JT. 2015. A comprehensive joint analysis of the long and short RNA transcriptomes of human erythrocytes. *BMC Genomics* **16:** 1–16. doi:10.1186/s12864-015-2156-2

Enuka Y, Lauriola M, Feldman ME, Sas-Chen A, Ulitsky I, Yarden Y. 2016. Circular RNAs are long-lived and display only minimal early alterations in response to a growth factor. *Nucleic Acids Res* **44:** 1370–1383. doi:10.1093/nar/gkv1367

Fischer JW, Busa VF, Shao Y, Leung AKL. 2020. Structure-mediated RNA decay by UPF1 and G3BP1. *Mol Cell* **78:** 70–84.e6. doi:10.1016/j.molcel.2020.01.021

Fiszbein A, Krick KS, Begg BE, Burge CB. 2019. Exon-mediated activation of transcription starts. *Cell* **179:** 1551–1565.e17. doi:10.1016/j.cell.2019.11.002

Gautier EF, Ducamp S, Leduc M, Salnot V, Guillonneau F, Dussiot M, Hale J, Giarratana MC, Raimbault A, Douay L, et al. 2016. Comprehensive proteomic analysis of human erythropoiesis. *Cell Rep* **16:** 1470–1484. doi:10.1016/j.celrep.2016.06.085

Goode DK, Obier N, Vijayabaskar MS, Lie-A-Ling M, Lilly AJ, Hannah R, Lichtinger M, Batta K, Florkowska M, Patel R, et al. 2016. Dynamic gene regulatory networks drive hematopoietic specification and differentiation. *Dev Cell* **36:** 572–587. doi:10.1016/j.devcel.2016.01.024

Guo JU, Agarwal V, Guo H, Bartel DP. 2014. Expanded identification and characterization of mammalian circular RNAs. *Genome Biol* **15:** 409. doi:10.1186/s13059-014-0409-z

Hansen TB. 2021. Signal and noise in circRNA translation. *Methods* **21:** 2020.12.10.418848.

Hansen TB, Jensen TI, Clausen BH, Bramsen JB, Finsen B, Damgaard CK, Kjems J. 2013. Natural RNA circles function as efficient microRNA sponges. *Nature* **495:** 384–388. doi:10.1038/nature11993

Hentze MW, Preiss T. 2013. Circular RNAs: splicing's enigma variations. *EMBO J* **32:** 923–925. doi:10.1038/emboj.2013.53

Heshusius S, Heideveld E, Burger P, Thiel-Valkhof M, Sellink E, Varga E, Ovchynnikova E, Visser A, Martens JHA, von Lindern M, et al. 2019. Large-scale in-vitro production of red blood cells from human peripheral blood mononuclear cells. *Blood Adv* **3:** 3337–3350. doi:10.1101/659862

Huang C, Liang D, Tatomer DC, Wilusz JE. 2018. A length-dependent evolutionarily conserved pathway controls nuclear export of circular RNAs. *Genes Dev* **32:** 639–644. doi:10.1101/gad.314856.118

Huang W, Ling Y, Zhang S, Xia Q, Cao R, Fan X, Fang Z, Wang Z, Zhang G. 2021. TransCirc: an interactive database for translatable circular RNAs based on multi-omics evidence. *Nucleic Acids Res* **49:** D236–D242. doi:10.1093/nar/gkaa823

Ingolia NT, Ghaemmaghami S, Newman JRS, Weissman JS. 2009. Genome-wide analysis in vivo of translation with nucleotide resolution using ribosome profiling. *Science* **324:** 218–223. doi:10.1126/science.1168978

Jeck WR, Sorrentino JA, Wang K, Slevin MK, Burd CE, Liu J, Marzluff WF, Sharpless NE. 2013. Circular RNAs are abundant, conserved, and associated with ALU repeats. *RNA* **19:** 141–157. doi:10.1261/rna.035667.112

Kelly S, Greenman C, Cook PR, Papantonis A. 2015. Exon skipping is correlated with exon circularization. *J Mol Biol* **427:** 2414–2417. doi:10.1016/j.jmb.2015.02.018

Kinsella RJ, Kähäri A, Haider S, Zamora J, Proctor G, Spudich G, Almeida-King J, Staines D, Derwent P, Kerhornou A, et al. 2011. Ensembl BioMarts: a hub for data retrieval across taxonomic space. *Database* **2011:** 1–9. doi:10.1093/database/bar030

Kissopoulou A, Jonasson J, Lindahl TL, Osman A. 2013. Next generation sequencing analysis of human platelet polyA+ mRNAs and rRNA-depleted total RNA. *PLoS One* **8:** e81809. doi:10.1371/journal.pone.0081809

Kolde R. 2012. Pheatmap: pretty heatmaps. https://cran.r-project.org/package=pheatmap.

Kristensen LS, Hansen TB, Venø MT, Kjems J. 2018. Circular RNAs in cancer: opportunities and challenges in the field. *Oncogene* **37:** 555–565. doi:10.1038/onc.2017.361

Legnini I, Di Timoteo G, Rossi F, Morlando M, Briganti F, Sthandier O, Fatica A, Santini T, Andronache A, Wade M, et al. 2017. Circ-ZNF609 is a circular RNA that can be translated and functions in myogenesis. *Mol Cell* **66:** 22–37.e9. doi:10.1016/j.molcel.2017.02.017

Li Z, Huang C, Bao C, Chen L, Lin M, Wang X, Zhong G, Yu B, Hu W, Dai L, et al. 2015. Exon-intron circular RNAs regulate transcription in the nucleus. *Nat Struct Mol Biol* **22:** 256–264. doi:10.1038/nsmb.2959

Li X, Liu C, Xue W, Zhang Y, Jiang S, Yin Q, Wei J, Yao R, Yang L, Chen L-L. 2017. Coordinated circRNA biogenesis and function with NF90/NF110 in viral infection. *Mol Cell* **67:** 214–227.e7. doi:10.1016/j.molcel.2017.05.023

Li X, Xiao L, Chung HK, Ma X-X, Liu X, Song J-L, Jin C, Rao JN, Gorospe M, Wang J. 2020. Interaction between HuR and circPABPN1 modulates autophagy in the intestinal epithelium by altering ATG16L1 translation. *Mol Cell Biol* **40:** e00492-19. doi:10.1128/MCB.00492-19

Liang WC, Wong CW, Liang PP, Shi M, Cao Y, Rao ST, Tsui SKW, Waye MMY, Zhang Q, Fu WM, et al. 2019. Translation of the

circular RNA circβ-catenin promotes liver cancer cell growth through activation of the Wnt pathway. *Genome Biol* **20:** 84. doi:10.1186/s13059-019-1685-4

Liu CX, Li X, Nan F, Jiang S, Gao X, Guo SK, Xue W, Cui Y, Dong K, Ding H, et al. 2019. Structure and degradation of circular RNAs regulate PKR activation in innate immunity. *Cell* **177:** 865–880. e21. doi:10.1016/j.cell.2019.03.046

Love MI, Huber W, Anders S. 2014. Moderated estimation of fold change and dispersion for RNA-seq data with DESeq2. *Genome Biol* **15:** 550. doi:10.1186/s13059-014-0550-8

Luo M, Jeong M, Sun D, Park HJ, Rodriguez BAT, Xia Z, Yang L, Zhang X, Sheng K, Darlington GJ, et al. 2015. Long non-coding RNAs control hematopoietic stem cell function. *Cell Stem Cell* **16:** 426–438. doi:10.1016/j.stem.2015.02.002

Maass PG, Gla P, Memczak S, Dittmar G, Hollfinger I, Schreyer L, Sauer A V, Toka O. 2017. A map of human circular RNAs in clinically relevant tissues. *J Mol Med* **95:** 1179–1189. doi:10.1007/s00109-017-1582-9

Martin M. 2011. Cutadapt removes adapter sequences from high-throughput sequencing reads. *EMBnet.journal* **17:** 10. doi:10.14806/ej.17.1.200

Martinez TF, Chu Q, Donaldson C, Tan D, Shokhirev MN, Saghatelian A. 2020. Accurate annotation of human protein-coding small open reading frames. *Nat Chem Biol* **16:** 458–468. doi:10.1038/s41589-019-0425-0

Memczak S, Jens M, Elefsinioti A, Torti F, Krueger J, Rybak A, Maier L, Mackowiak SD, Gregersen LH, Munschauer M, et al. 2013. Circular RNAs are a large class of animal RNAs with regulatory potency. *Nature* **495:** 333–338. doi:10.1038/nature11928

Mills EW, Wangen J, Green R, Ingolia NT. 2016. Dynamic regulation of a ribosome rescue pathway in erythroid cells and platelets. *Cell Rep* **17:** 1–10. doi:10.1016/j.celrep.2016.08.088

Nassa G, Giurato G, Cimmino G, Rizzo F, Ravo M, Salvati A, Nyman TA, Zhu Y, Vesterlund M, Lehtiö J, et al. 2018. Splicing of platelet resident pre-mRNAs upon activation by physiological stimuli results in functionally relevant proteome modifications. *Sci Rep* **8:** 498. doi:10.1038/s41598-017-18985-5

Nicolet BP, Engels S, Aglialoro F, van den Akker E, von Lindern M, Wolkers MC. 2018. Circular RNA expression in human hematopoietic cells is widespread and cell-type specific. *Nucleic Acids Res* **46:** 8168–8180. doi:10.1093/nar/gky721

Notta F, Zandi S, Takayama N, Dobson S, Gan OI, Wilson G, Kaufmann KB, McLeod J, Laurenti E, Dunant CF, et al. 2016. Distinct routes of lineage development reshape the human blood hierarchy across ontogeny. *Science* **351:** aab2116. doi:10.1126/science.aab2116

Pamudurti NR, Bartok O, Jens M, Ashwal-Fluss R, Stottmeister C, Ruhe L, Hanan M, Wyler E, Perez-Hernandez D, Ramberger E, et al. 2017. Translation of CircRNAs. *Mol Cell* **66:** 9–21.e7. doi:10.1016/j.molcel.2017.02.021

Patro R, Duggal G, Love MI, Irizarry RA, Kingsford C. 2017. Salmon provides fast and bias-aware quantification of transcript expression. *Nat Methods* **14:** 417–419. doi:10.1038/nmeth.4197

Petriv OI, Kuchenbauer F, Delaney AD, Lecault V, White A, Kent D, Marmolejo L, Heuser M, Berg T, Copley M, et al. 2010. Comprehensive microRNA expression profiling of the hematopoietic hierarchy. *Proc Natl Acad Sci* **107:** 15443–15448. doi:10.1073/pnas.1009320107

Piwecka M, Glažar P, Hernandez-Miranda LR, Memczak S, Wolf SA, Rybak-Wolf A, Filipchyk A, Klironomos F, Cerda Jara CA, Fenske P, et al. 2017. Loss of a mammalian circular RNA locus causes miRNA deregulation and affects brain function. *Science* **8526:** eaam8526. doi:10.1126/science.aam8526

Quinlan AR, Hall IM. 2010. BEDTools: a flexible suite of utilities for comparing genomic features. *Bioinformatics* **26:** 841–842. doi:10.1093/bioinformatics/btq033

Rybak-Wolf A, Stottmeister C, Glažar P, Jens M, Pino N, Giusti S, Hanan M, Behm M, Bartok O, Ashwal-Fluss R, et al. 2015. Circular RNAs in the mammalian brain are highly abundant, conserved, and dynamically expressed. *Mol Cell* **58:** 870–885. doi:10.1016/j.molcel.2015.03.027

Stagsted LV, Nielsen KM, Daugaard I, Hansen TB. 2019. Noncoding AUG circRNAs constitute an abundant and conserved subclass of circles. *Life Sci Alliance* **2:** e201900398. doi:10.26508/lsa.201900398

Sun YM, Wang WT, Zeng ZC, Chen TQ, Han C, Pan Q, Huang W, Fang K, Sun LY, Zhou YF, et al. 2019. CircMYBL2, a circRNA from MYBL2, regulates FLT3 translation by recruiting PTBP1 to promote FLT3-ITD AML progression. *Blood* **134:** 1533–1546. doi:10.1182/blood.2019000802

Suzuki H, Zuo Y, Wang J, Zhang MQ, Malhotra A, Mayeda A. 2006. Characterization of RNase R-digested cellular RNA source that consists of lariat and circular RNAs from pre-mRNA splicing. *Nucleic Acids Res* **34:** e63. doi:10.1093/nar/gkl151

Van Oorschot R, Hansen M, Koornneef JM, Marneth AE, Bergevoet SM, Van Bergen MGJM, Van Alphen FPJ, Van Der Zwaan C, Martens JHA, Vermeulen M, et al. 2019. Molecular mechanisms of bleeding disorderassociated GFI1BQ287* mutation and its affected pathways in megakaryocytes and platelets. *Haematologica* **104:** 1460–1472. doi:10.3324/haematol.2018.194555

Wei T, Simko V. 2017. *R package "corrplot": visualization of a correlation matrix*, version 0.84. https://github.com/taiyun/corrplot

Westholm JO, Miura P, Olson S, Shenker S, Joseph B, Sanfilippo P, Celniker SE, Graveley BR, Lai EC. 2014. Genome-wide analysis of *Drosophila* circular RNAs reveals their structural and sequence properties and age-dependent neural accumulation. *Cell Rep* **9:** 1966–1980. doi:10.1016/j.celrep.2014.10.062

Wickham H. 2016. *ggplot2: elegant graphics for data analysis*. Springer-Verlag New York, New York, NY.

Wu N, Yuan Z, Du KY, Fang L, Lyu J, Zhang C, He A, Eshaghi E, Zeng K, Ma J, et al. 2019. Translation of yes-associated protein (YAP) was antagonized by its circular RNA via suppressing the assembly of the translation initiation machinery. *Cell Death Differ* **26:** 2758–2773. doi:10.1038/s41418-019-0337-2

Yang Y, Fan X, Mao M, Song X, Wu P, Zhang Y, Jin Y, Yang Y, Chen L-L, Wang Y, et al. 2017. Extensive translation of circular RNAs driven by N6-methyladenosine. *Cell Res* **27:** 626–641. doi:10.1038/cr.2017.31

Zhang XO, Bin WH, Zhang Y, Lu X, Chen LL, Yang L. 2014. Complementary sequence-mediated exon circularization. *Cell* **159:** 134–147. doi:10.1016/j.cell.2014.09.001

Zhang Y, Xue W, Li X, Zhang J, Chen S, Zhang JL, Yang L, Chen LL. 2016. The biogenesis of nascent circular RNAs. *Cell Rep* **15:** 611–624. doi:10.1016/j.celrep.2016.03.058

See the following page for ***Meet the First Author***

MEET THE FIRST AUTHOR

Benoit P. Nicolet

***Meet the First Author(s)* is a new editorial feature within *RNA*, in which the first author(s) of research-based papers in each issue have the opportunity to introduce themselves and their work to readers of *RNA* and the RNA research community. Benoit Nicolet is the first author of this paper, "Circular RNAs exhibit limited evidence for translation, or translation regulation of the mRNA counterpart in terminal hematopoiesis." Benoit is a postdoc in the laboratory of Monika Wolkers at Sanquin Blood Foundation in Amsterdam, the Netherlands, who studies the regulation of gene expression in blood cells, mostly T lymphocytes, with a focus on post-transcriptional events.**

What are the major results described in your paper and how do they impact this branch of the field?

CircRNAs are quite mysterious molecules that are amply expressed in cells. Yet their cellular role remains enigmatic. Here we studied whether endogenously expressed circRNAs associate with translation regulation, or if they can be translated. Despite their very high expression levels in terminally differentiated human blood cells, we found very little evidence that circRNAs regulate translation of their mRNA counterparts, or that circRNAs are translated. This last finding contrasts with that of exogenous circRNAs over-expression constructs in cells. I therefore would like to highlight that endogenously expressed circRNAs appear to act differently and are in fact seldomly translated, if at all.

What led you to study RNA or this aspect of RNA science?

To be honest, serendipity and finding circRNA biology "cool" got me into this topic. I was at a conference attending a talk on circRNAs. Primed by this excellent talk, I searched for studies on circRNAs in blood cells. At that time, I could not find one single report. Yet, we had all the data sets compatible to address that very lack of information. After a little bit of setup, I found the expression of circRNAs in blood cells, and in particular in platelets and red blood cells, is very high. Why was that? I was hooked.

During the course of these experiments, were there any surprising results or particular difficulties that altered your thinking and subsequent focus?

I started with the hypothesis that I would see thousands of the circRNAs being translated in blood cells. To me this was in particular an exciting thought for red blood cells and platelets, which lack de novo RNA transcription. Thus, the intrinsic stability of circRNAs could possibly provide the templates for translation. This would have been further supported by the finding that circRNA expression massively increases around enucleation. However, as you can read in our paper, endogenous circRNAs are not at all widely translated.

What are your subsequent near- or long-term career plans?

Haha, good one. I guess wherever my interests take me. I would like to combine machine learning with biological measurements (omics) to better understand gene expression in cells. I am also a cofounder of Green Labs Netherlands (Green Labs NL) and the Sustainable European Laboratories (SELs), two networks trying to make science just as fun, but more sustainable. Let's see how things develop!